L B Gardner / JA64

MRI REPORT

CONTAINERLESS HIGH TEMPERATURE PROPERTY MEASUREMENTS BY ATOMIC FLUORESCENCE

ANNUAL TECHNICAL REPORT
June 1983

NASA Contract No. NAS8-34383
MRI Project No. RA-314-G

Prepared for

Materials Processing in Space Program
Contract Monitor: L. B. Gardner, JA64
NASA-George C. Marshall Space Flight Center
Marshall Space Flight Center, Alabama 35812

CONTAINERLESS HIGH TEMPERATURE PROPERTY MEASUREMENTS BY ATOMIC FLUORESCENCE

ANNUAL TECHNICAL REPORT
June 1983

NASA Contract No. NAS8-34383
MRI Project No. RA-314-G

Prepared for

Materials Processing in Space Program
Contract Monitor: L. B. Gardner, JA64
NASA-George C. Marshall Space Flight Center
Marshall Space Flight Center, Alabama 35812

MIDWEST RESEARCH INSTITUTE 425 VOLKER BOULEVARD KANSAS CITY MISSOURI 64110 • 816 753 7600

PREFACE

This is the second annual report for NASA Contract No. NAS8-34383 with Yale University. Since November 1, 1982, a portion of the work, including reporting requirements, has been subcontracted by Yale University to Midwest Research Institute, where the principal investigator, P. C. Nordine, is now employed. Dr. R. A. Schiffman and Prof. C. A. Walker of Yale University are co-principal investigators for the contract.

Dr. Nordine is the appropriate contact concerning technical and administrative questions about the work.

Approved:

MIDWEST RESEARCH INSTITUTE

for L. J. Shannon, Executive Director
Engineering and Applied Sciences Group

TABLE OF CONTENTS

		Page
I.	Introduction	1
II.	Experimental	3
III.	Results	6
	1. Al_2O_3 (alumina and sapphire)	6
	2. Gas Density Thermometry	8
	3. Properties of Levitation Jets	10
	4. Molybdenum Evaporation	10
IV.	Discussion	25
V.	References	29
VI.	Publications and Presentations	30
VII.	Distribution	31

List of Figures

Figure	Title	Page
1a	Side View of the Experiment.	4
1b	Top View of the Apparatus.	4
2	Al-Atom Fluorescence Intensity versus Apparent Temperature for Levitated 4 mm and 5 mm Sapphire Spheres. . . .	7
3	Al-Atom Fluorescence Intensity versus Apparent Temperature for Levitated 3.18 mm Polycrystalline Alumina (A,B) and Sapphire (C,D) Spheres	9
4	Axial Variation of Hg-Seed Atom Concentration in a Supersonic Free Jet of Argon Gas	11
5	Laser Induced Hg-Atom Fluorescence Photographs of Supersonic Free Jets of Mercury Seeded Argon Gas.	12
6	Temperature Dependence of Mo ($^7S_3$) Ground State Fluorescent Intensity over Electromagnetically Levitated, CW CO_2 Laser Heated Molybdenum Spheres, in Vacuum	13
7	Partial Energy Level Diagram for Atomic Tungsten	16
8	Radiative Lifetimes for Atomic Tungsten.	17
9	Temperature Dependence of Fluorescence Intensity for W ($^5D_0$) Ground State Atoms in the Wake of an Electrically Heated Tungsten Filament.	18
10	Temperature Dependence of Fluorescent Intensity for Five Electronic States of Atomic Tungsten in the Wake of Electrically Heated Tungsten Filaments	20
11	Measurement of the $^3P_0:^5D_0$ Fluorescence Intensity Ratio. .	21
12	Temperature Dependence of the Tungsten Ion Ground State Fluorescence Intensity in the Wake of an Electrically Heated Tungsten Filament	24

List of Tables

Table	Title	Page
1	Atom Pressures and Specimen Temperatures	5
2	Species Detected by Laser Induced Fluorescence	5
3	Tungsten Filament Evaporation Results.	22

1. INTRODUCTION

This research is directed to the use of laser induced fluorescence (LIF) techniques for containerless study of high temperature processes and material properties. Gas jet and electromagnetic levitation and electromagnetic and laser heating techniques are used with LIF in earth-based containerless high temperature experiments. The work to date includes development of an apparatus and its use in studies of (a) chemical reactions on Al_2O_3, molybdenum, and tungsten specimens, (b) novel methods for noncontact specimen temperature measurement, and (c) levitation jet properties. Brief summaries of these studies are given below. The apparatus is described in Section II and detailed results for the current reporting period are presented in Section III. Previous work was presented in our first annual report.[1]

1. Al_2O_3 (sapphire and alumina) evaporation: Al-atom evaporation from Al_2O_3 specimens was studied at temperatures up to 2327K, the melting point of Al_2O_3, using CW CO_2 laser heated sapphire and polycrystalline alumina specimens that were levitated in a gas jet and a self-supported sapphire filament specimen. The experiments yield accurate optical properties that are needed for temperature measurements. The emittance of alumina was found to increase with the ambient oxygen partial pressure. The effective emittance of nearly transparent sapphire is directly proportional to the specimen thickness. LIF sensitivity is sufficient that Al-atom concentrations as small as 2×10^8 cm^{-3} can be measured with F-15 light collecting optics. A 100-fold increase in sensitivity would be possible if a small F-No lens were used to collect fluorescence.

2. Gas density thermometry:[1] A new method for noncontact temperature measurement on transparent specimens was demonstrated by adding mercury atoms to the Ar gas flow in which Al_2O_3 specimens were levitated and heated, and measuring Hg-atom concentrations near the specimen surfaces relative to the concentration under ambient conditions. The ambient temperature to high temperature Hg-atom concentration ratios (obtained by LIF) increase with specimen temperature and show a different dependence on apparent temperature for the two materials, due to their different emittances. When the optical properties of alumina and sapphire are taken into account, gas density versus temperature functions are the same for both specimens. Thus, LIF measurements of gas density on a material of known emittance (and known temperature via optical pyrometry) yield a density versus temperature function that may subsequently be used to measure temperatures on materials whose optical properties are not known or change during a process. The precision achieved in LIF gas density thermometry was about ±3%. The relation between ambient and high temperature Hg-atom concentration is influenced by the relative magnitudes of transport by convection and thermal diffusion. Reduced convection rates and smaller temperature gradients in space-based experiments would permit more precise and accurate use of this method than is possible on earth.

3. Properties of levitation jets: The most successful arrangement for high temperature gas jet levitation experiments employs a supersonic free jet to levitate the heated specimen.[2,3] The properties of such jets were studied by measuring LIF of Hg atoms added to the argon flow. Velocity measurements were achieved[1] by measuring the fluorescent image position versus delay time between laser excitation and fluorescence detection. The jet shock structure was measured by laser induced fluorescence photography and by electronic measurement of the radial and axial variations of Hg-atom density in the jet. The results provide independent support for our earlier conclusions[2] about levitation jet behavior that were based on levitation height versus flow rate and pressure experiments and on pitot tube measurements of jet properties. These results establish the sensitivity, precision, and spatial resolution with which velocities and nonuniform concentrations can be measured by these LIF techniques.

4. Molybdenum evaporation: Molybdenum specimens were inductively levitated and laser heated in vacuum in the temperature range 2110 to 2790K. LIF intensity was measured versus temperature between 2290 and 2770K by exciting ground state $^7S_3$ Mo atoms to the $^3P_4^o$ level at λ = 379.8 nm. The enthalpy of molybdenum evaporation to the atomic ground state, ΔH_T^o = 610 ± 15 kJ/g-mole, was derived from a plot of ln(IT) versus 1/T. This result is in good agreement with the value (ΔH_T^o = 631 ± 2 kJ/g-mole) derived from the accepted thermodynamic properties of molybdenum.[4] The intensity versus temperature data revealed that self-absorption of LIF occurs at the highest temperatures and a model of the self-absorption process was employed in the data reduction. Accurate self-absorption corrections are possible if this effect reduces LIF intensity by no more than a factor of two.

5. Tungsten evaporation: Tungsten filament evaporation was studied in the temperature range 2740 to 3680K, the melting point of tungsten. The experiments were carried out in a flow of argon gas at p = 190 Pa. Nine different metastable electronic states of atomic W were detected and intensity versus temperature data obtained for five of these states. Tungsten ions were also detected. The average derived value for the enthalpy of solid tungsten evaporation to ground state atoms at T = 3120K was 861 ± 24 kJ/g-mole, which slightly exceeds the accepted value (826 ± 4 kJ/g-mole) for this property. The difference is in part due to an increase with specimen temperature in the proportionality constant that relates intensity to specimen vapor pressure, which cannot be accurately calculated in these flow reactor experiments. This problem does not arise in vacuum evaporation experiments and can also be avoided in levitation experiments at higher inert gas pressures for which boundary layer transport rates and gradients would be small.

The tungsten atom $^5D_0$:$^3P_0$ concentration ratios were obtained versus temperature by measuring fluorescence when atoms in these states were excited to the same upper level. The concentration ratios measured in this way are free from self-absorption and other effects that influence the relation between intensity and specimen vapor pressure. The correct $^5D_0$ - $^3P_0$ excitation energy was derived from the intensity ratio measurements. Such measurements provide a promising method by which the specimen temperature may be obtained if two lasers are used for simultaneous concentration measurements for two different atomic electronic states.

II. EXPERIMENTAL

The apparatus used in this research is illustrated in Figures 1a and 1b, for which the components are identified in the figure captions. In the experiments reported, a pulsed dye laser was used to produce fluorescence from atomic mercury, aluminum, molybdenum, tungsten, and tungsten ions. The Hg atoms were added to the argon flow. Al atoms were produced by evaporation from CW CO_2 laser heated and aerodynamically levitated sapphire and polycrystalline alumina spheres or self-supported sapphire filaments. Mo atoms were evaporated from solid spheres that were inductively levitated and laser heated in vacuum. W atoms and ions were evaporated from electrically heated metal filaments.

Electromagnetic induction levitation experiments with tungsten, molybdenum, and zirconium specimens were achieved. A 2.5 kW, 450 KHz power supply was used with levitation coil designs similar to those of Van Audenhove.[12] CW CO_2 laser heating of the levitated Mo and W specimens was also investigated. Levitated 2.5 mm diameter Mo spheres were just heated to the melting point at maximum laser power (ca. 300 W). Smaller Mo spheres were levitated at lower temperatures but became unstable and fell from the levitation coil as the temperature was increased. Stable levitation of tungsten could not be achieved at temperatures above about 3000K. Liquid Zr was levitated and electromagnetically heated to about 2400K, at which temperature the specimens fell from the levitation coil. Specimens larger than about 3 mm diameter were not investigated.

The apparatus includes a second harmonic generation cell (SHG cell) that doubles the dye laser output frequency for fluorescence studies at λ = 220 - 360 nm. This cell is angle-tuned and efficiently doubles only the central component of the dye laser beam. Radiation diffracted from surfaces and apertures in the dye laser is not doubled by the SHG cell. The spatial mode of the frequency doubled beam is more perfect than that of the dye laser. The frequency doubled beam can thus be focused to a nearly diffraction limited spot, which is not possible with the direct dye laser beam, and superior spatial resolution in fluorescence intensity measurements was achieved only with the frequency doubled beam. A spatial filter that would yield good focusing properties for the dye laser beam has not been installed.

Table 1 lists the atom vapor pressures and specimen temperatures under which LIF measurements were carried out. Even smaller vapor pressures (by about a factor of 100) could be measured with a smaller F-No light collecting lens. Electronic states of the detected species are given in Table 2, along with their electronic excitation energies and the laser wavelengths at which fluorescence was excited.

In a separate experiment, an F2.5 lens, 300 ± 100 nm interference filter (transmission > 50% at 253.7 nm) and a Polaroid camera (with Polaroid 084, ASA 3000 film) were used to obtain a photographic image of levitation jets by Hg-atom LIF. The laser beam was focused to a diameter ca. 0.025 cm at the center for the jet and swept up and down along the jet axis with the camera shutter open to expose the photograph.

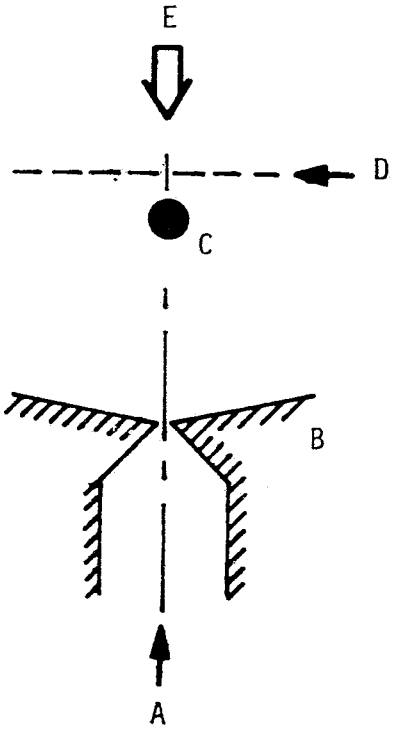

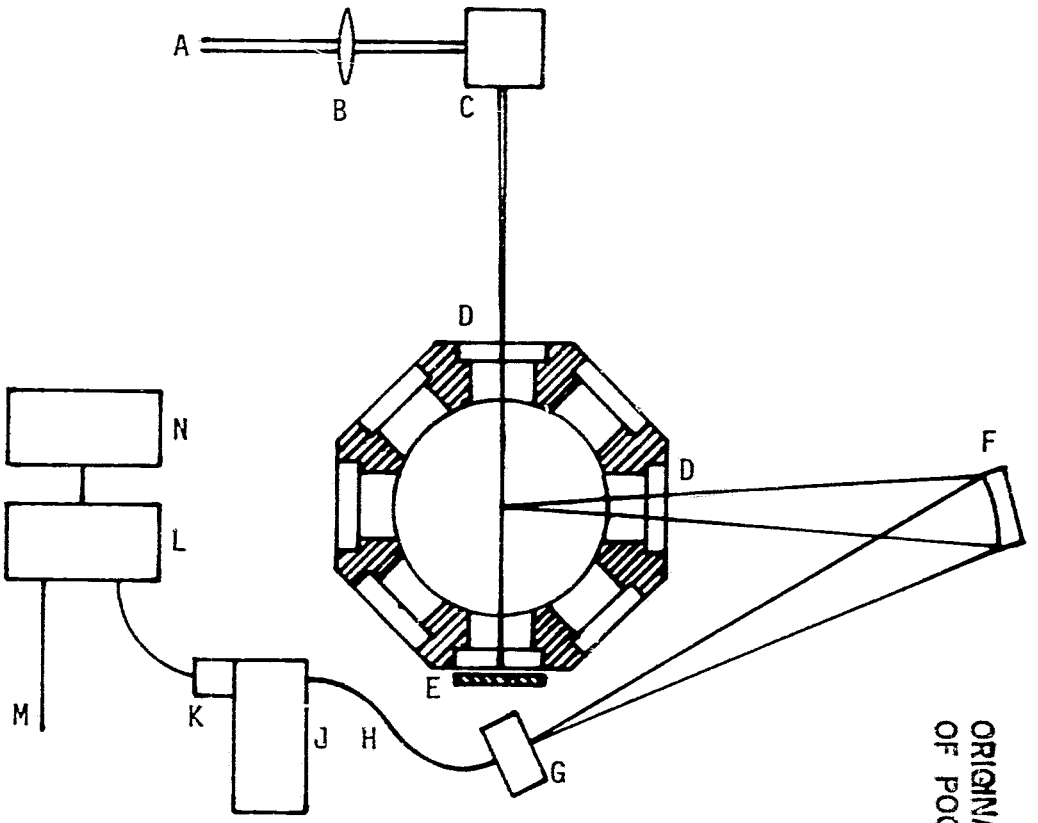

Figure 1a (left) - Side View of the Experiment. A - Ar flow, with added Hg, B - Nozzle with 0.082 cm diameter throat, C - Levitated specimen D - Focused dye laser beam, E - CW CO_2 heating laser.

Figure 1b (right) - Top View of the Apparatus. A - Pulsed laser beam, B - Quartz lens, focal length = 50 cm, C - Beam steering device, D - Quartz windows, E - Laser beam stop, F - Front surface reflective lens, G - 0.40 mm aperture and positioning device, H - uv grade optical fiber, J - 1/4 m monochromator, K - Phototube, L - Boxcar averager, M - Trigger signal from laser, N - Chart recorder.

TABLE 1

ATOM PRESSURES[4,5] AND SPECIMEN TEMPERATURES

Species	Pressure, atm.	Temperature (°K)
Al	2.0E-10 to 1.0E-6	1830 - 2327
Mo	1.1E-9 to 1.6E-5	2070 - 2790
W	3.6E-9 to 5.0E-5	2750 - 3680
W+		2860 - 3420
Hg	~ 4 E-7	298 - 2327

TABLE 2

SPECIES DETECTED BY LASER INDUCED FLUORESCENCE

Species	Term[9]	Energy,[9] (kJ/g-mole)	Laser Wavelengths[10] (nm)
Al	$^2P_{1/2}$	0	256.8, 265.2, 308.2, 394.4
	$^2P_{3/2}$	1.3	257.5, 266.0, 309.3, 396.2
Mo	$^7S_3$	0	379.8
W	$^5D_0$	0	291.1, 384.7
	$^5D_1$	20.0	400.5, 505.2
	$^7S_3$	35.3	400.9, 404.6
	$^5D_2$	39.8	484.4, 597.3
	$^5D_4$	74.4	396.5, 488.7
	$^3P_0$	114.0	402.9
	H_4	145.5	397.5, 400.1
	$^2G_3$	159.7	404.7, 405.5
	$^2H_5$	180.3	407.3
W+	$^6D_{1/2}$	0	255.5
Hg	$^1S_0$	0	253.7

III. RESULTS

This section presents new results for the current reporting period. Brief summaries of earlier work are included.

1. Al_2O_3 (alumina and sapphire): In the earlier Al-atom fluorescence experiments[1] it was found that the Al intensity increases with apparent temperature up to the melting point of the specimen. At the melting point, the apparent temperature continues to increase as the fraction of the specimen that is liquid increases, due to a larger emittance for the liquid than for the solid. The true temperature (2327K) and the Al-atom intensity remain constant for partially molten specimens. The temperature dependence of specimen emittance is calculated from the Al-atom fluorescence intensity measurements, the apparent melting temperature, and the known variation of Al-atom vapor pressure with temperature over Al_2O_3.

Figure 2 presents intensity versus temperature data obtained with 4- and 5-mm sapphire specimens. The intensities have been adjusted so that the maximum intensity for the 4-mm specimen is twice that for the 5-mm specimen. The two curves are parallel and the reciprocal temperature difference at equal fractions of the maximum intensity is

$$\Delta(1/T) = (1.1 + 0.1) \times 10^{-5}\ K^{-1} \qquad (1)$$

This result indicates that the emittance of sapphire is proportional to specimen thickness. Then the reciprocal temperature difference would be

$$\Delta(1/T) = (\lambda/C_2)\ \ln(d_2/d_1). \qquad (2)$$

With $\lambda = 0.66\ \mu$, $C_2 = 14{,}388\ \mu K$, $d_2 = 5$ mm, and $d_1 = 4$ mm, Eq. (2) gives $\Delta(1/T) = 1.02 \times 10^{-5}\ K^{-1}$, in agreement with the experimental result.

The slope of the ln(I) versus $1/T_a$ curves in Figure 2 is:

$$d\ \ln(I)/d(1/T_a) = -112{,}000\ K. \qquad (3)$$

An approximate calculation which assumes that the major species (Al and O) are the only gaseous species over Al_2O_3* gives, from known thermodynamic properties[5]

$$d\ \ln(I)/d(1/T) = -70{,}889\ K, \qquad (4)$$

where intensity, I, is proportional to the equilibrium Al-atom concentration over Al_2O_3. The normal spectral emittance, ε_λ, of 5-mm sapphire is obtained from its apparent melting temperature, $T_a = 1511K$, the true melting temperature, $T = 2327K$,[5] and the equation:

$$1/T_a - 1/T = -(\lambda/C_2)\ln\varepsilon_\lambda \qquad (5)$$

* AlO_2, AlO, Al_2O, Al_2O_2, and O_2 are minor species[5] in the vapor over Al_2O_3.

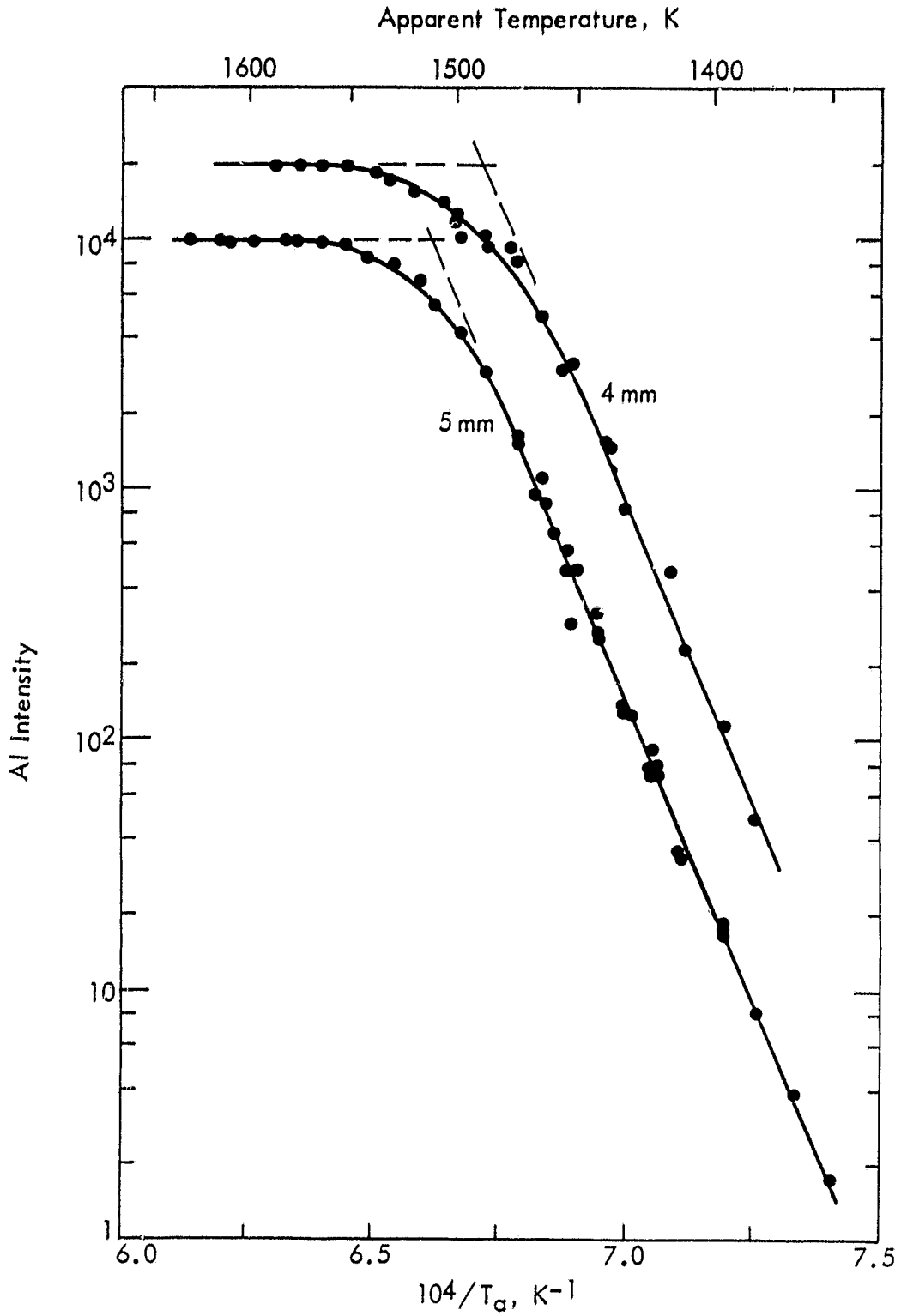

Figure 2 - Al-Atom Fluorescence Intensity versus Apparent Temperature for Levitated 4 mm and 5 mm Sapphire Spheres

which gives $\varepsilon_\lambda = 6.4 \times 10^{-3}$ at the melting point of the 5-mm sapphire sphere. From these results we obtain

$$1/T_a = 0.633/T + 3.90 \times 10^{-4}\ K^{-1} \qquad (6)$$

for the 5-mm specimen in the temperature range 1800 to 2327K. The emittance of sapphire spheres is then given by

$$\varepsilon(\lambda = 0.66\ \mu)/d(cm) = 4.08 \times 10^{-4} \exp(8002/T). \qquad (7)$$

This result indicates that the spectral emittance of sapphire decreases with temperature above 1800K, in agreement with the spectral absorption coefficient measurements of Grvnak and Burch.[6] They found $K_\lambda = 0.036$/cm at 1973K and $K_\lambda = 0.028$/cm at 2273K (and $\lambda = 0.66\ \mu$). These values are in good agreement with absorption coefficients calculated from Eq. (7), with $\varepsilon/d \cong K_\lambda$.

Figure 3 presents intensity versus apparent temperature data for sapphire and alumina, measured in argon and in oxygen-seeded argon on the same specimens. The lower intensities observed in oxygen-seeded argon result from the reaction of evaporating Al atoms with gaseous O_2 in the region between the specimen surface and the point at which laser induced fluorescence is observed. The fractional intensity decrease should increase with the rate constant for Al/O_2 reaction. Since this decrease is constant for the sapphire experiment, it is clear that the Al/O_2 rate constant is nearly independent of temperature.

The apparent melting point derived for the oxygen-seeded sapphire experiment agrees with that in argon, but the apparent melting point of polycrystalline alumina increases from 1800 ± 20K in argon to 1890 ± 20K in oxygen-seeded argon. Thus, it appears that the emittance of polycrystalline alumina depends on the ambient oxygen concentration. This result provides an explanation for the relatively low apparent melting temperatures for alumina in the present experiments, compared with the much higher value (2270 ± 20K) measured on laser heated alumina rods in air.[7]

2. Gas density thermometry:[1] Laser induced fluorescence measurements of temperature by gas density thermometry may be achieved by measuring the concentration of atomic Hg near a hot specimen and at another location in the system, where the temperature is known. This idea was evaluated by measuring Hg-atom fluorescent intensities in a levitation jet and in the wake of levitated and laser heated alumina and sapphire spheres versus the apparent temperature of the specimen. Different density ratio versus apparent temperature functions were obtained for the two specimens due to the different spectral emittances of alumina and sapphire. The appropriate corrections to the apparent sapphire temperatures were equal to those obtained from the Al-atom intensity versus temperature measurements over the same specimens.

The precision of temperatures obtained by gas density thermometry was ca. ± 3% in these experiments, with sapphire and alumina specimens of nearly equal mass and diameter and under nearly identical levitation gas

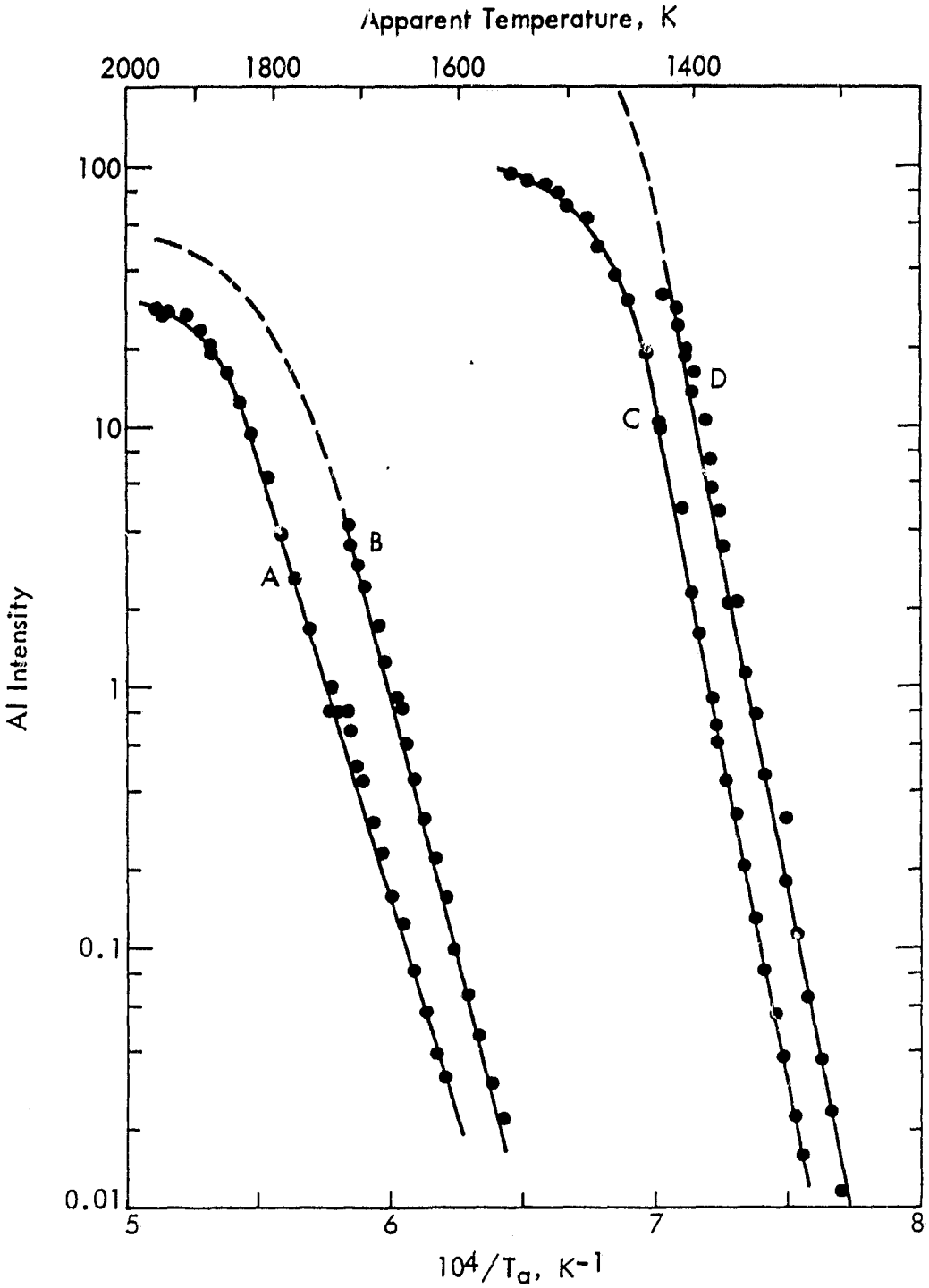

Figure 3 - Al-Atom Fluorescence Intensity versus Apparent Temperature for Levitated 3.18 mm Polycrystalline Alumina (A,B) and Sapphire (C,D) Spheres. A,C - $p(O_2) \cong 1$ Pa. B,D - $p(O_2) = 0$.

flow rates and ambient pressures. Thermal diffusion effects influence the measured density ratios, by amounts that depend on the gas flow rates and ambient pressures, and the method would not be easily applied to other levitation experiments. However, for containerless experiments in space, where negligible convective effects can be achieved in nonisothermal experiments, this method of gas density thermometry should provide accurate absolute temperature measurements. Large temperature gradients in the wake of levitated specimens, and small variations in the position of the specimen were major contributors to scatter of temperature measurements in the present experiments. In space, reduced convection rates would yield smaller temperature gradients and allow gas density temperature measurements whose precision exceeds that (±3%) achieved here.

3. Properties of levitation jets: The properties of levitation jets were studied by measuring spatially resolved Hg-atom fluorescence intensities in the Hg-seeded argon levitation jet. The volume from which fluorescence was collected was ca. $(0.03\ cm)^3$, and its location was measured to ± 0.001 cm. In our earlier work,[1] jet velocities were obtained from the location of the fluorescent image versus the delay time between the laser pulse and intensity measurement. Delay times up to 250 ns were possible at the 120-ns radiative lifetime of Hg ($^3P_1$) atoms, and velocities were measured to ± 24 m/s. Radial variations of density in the levitation jets were also obtained. The Hg concentration at the jet center was measured relative to the ambient concentration versus the nozzle pressure ratio. The density ratios so obtained agree with values calculated from an earlier study[2] of levitation jets by pitot tube pressure measurements and levitation height versus pressure measurements.

Figure 4 presents the variation of density in the jet (relative to the ambient density) versus height, Z, above the nozzle. The free jet expansion process produces a strong shock at Z ~ 3 mm from the nozzle and a series of weaker shocks further downstream. Fluorescence photographs of the jet are presented in Figure 5, for nozzle stagnation pressures and pressure ratios stated in the figure caption. The argon flow rates (in g/s) for these experiments equal 8.98×10^{-7} times the nozzle stagnation pressures (in Pa). Figures 5A-C show the shock spacing, ΔZ, increases as the nozzle pressure ratio (p_0/p) increases, in good agreement with the expected[8] result:

$$\Delta Z/d_n \simeq 0.67\ (p_0/p)^{1/2} \qquad (8)$$

where d_n is the nozzle diameter (0.062 cm). The images in Figures 5A-C were obtained with a slightly larger flow rate than that required to levitate alumina spheres. Figures 5D-F illustrate the effects of flow rate on the jet structure at a constant nozzle pressure ratio. Although the shock spacing remains constant, the greater effects of viscosity at smaller flow rates are evident in the far field of the jets.

4. Molybdenum evaporation: Figure 6 presents the intensity versus temperature data obtained on electromagnetically levitated molybdenum spheres.

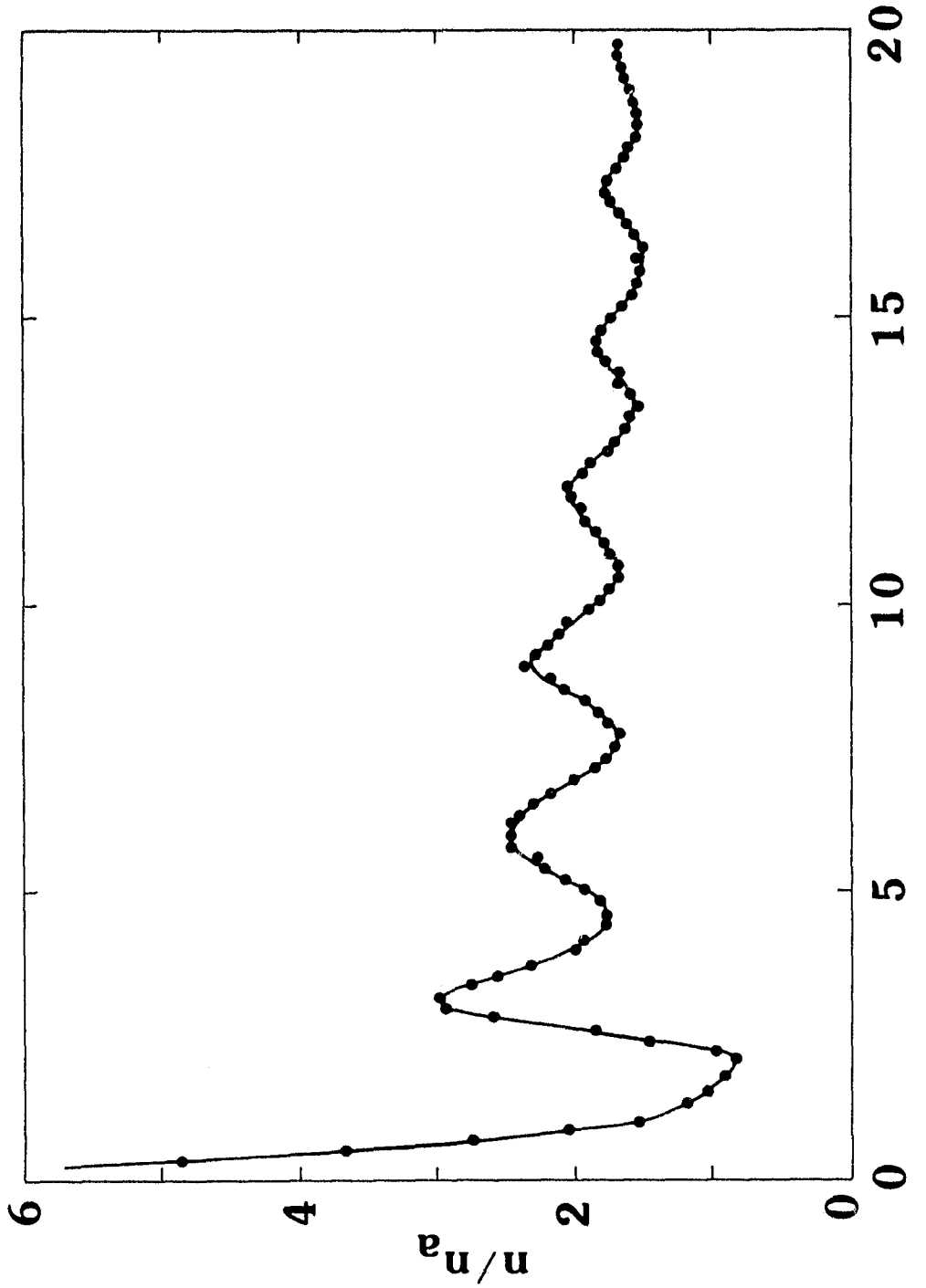

Figure 4 - Axial Variation of Hg-Seed Atom Concentration in a Supersonic Free Jet of Argon Gas. Conditions are: Ar flow rate = 13.6 mg/s, P_o = 15,100 Pa, P = 460 Pa. The nozzle, whose effective diameter is 0.062 cm is located at z = 0.

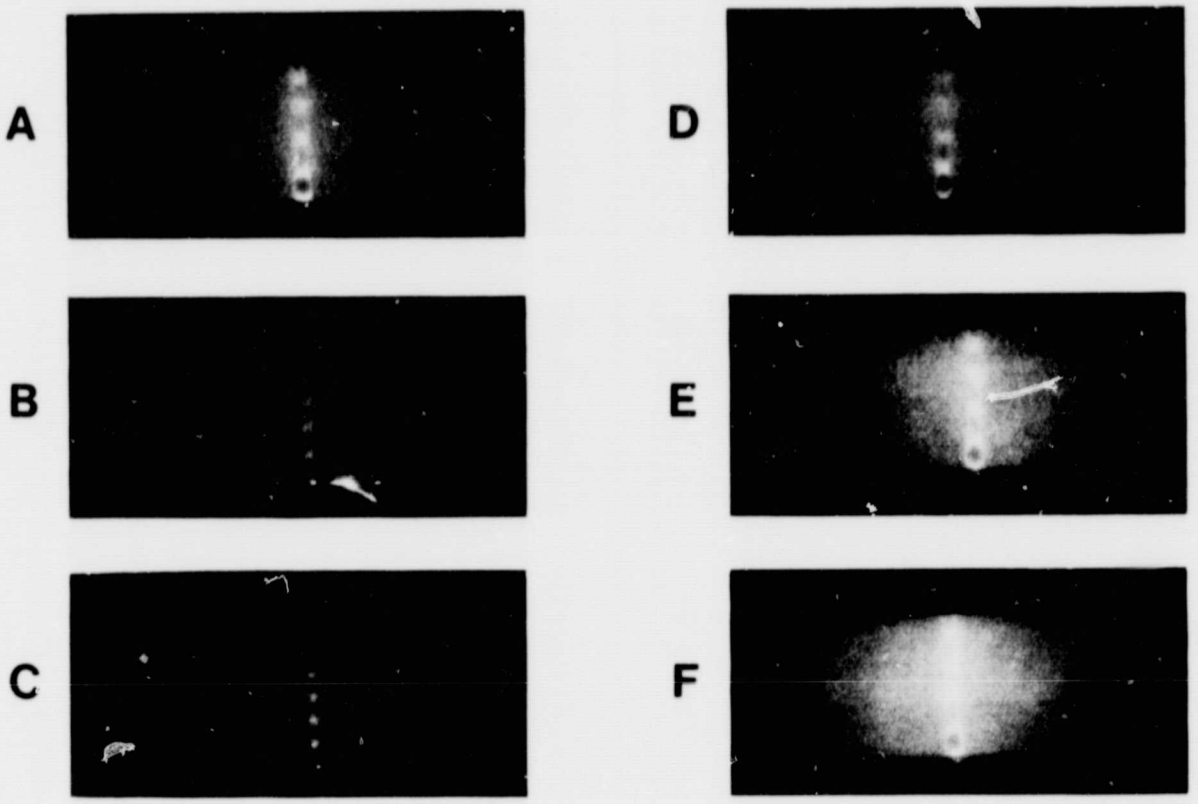

Figure 5 - Laser Induced Hg-Atom Fluorescence Photographs of Supersonic Free Jets of Mercury Seeded Argon Gas. Actual height of the imaged region was 1.34 cm. Reflection from the nozzle is apparent at the bottom of panel B. The effective nozzle throat diameter was 0.062 cm. Nozzle stagnation pressures (Pa): A,B,C,E - 15,000; D-7,400; F-27,500. Nozzle pressure ratios: A,D,E,F-33; B-21; C-15.

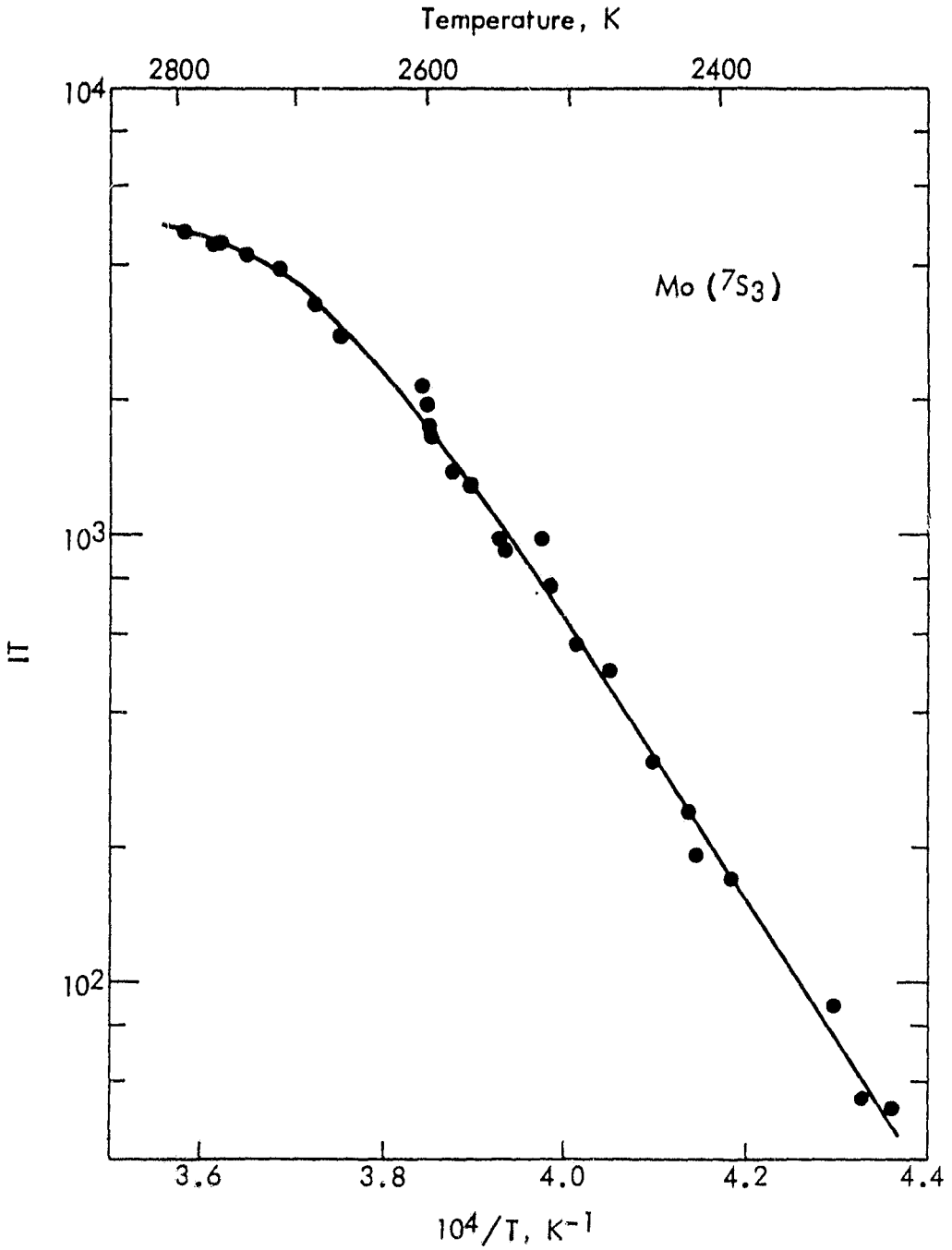

Figure 6 - Temperature Dependence of Mo ($^7S_3$) Ground State Fluorescent Intensity over Electromagnetically Levitated, CW CO_2 Laser Heated Molybdenum Spheres, in Vacuum.

The plot of ln(IT) versus 1/T is chosen to present these results because intensity is proportional to atom number density, and IT is proportional to the Mo-atom pressure. If this proportionality is maintained, the vaporization enthalpy can be calculated from the slope of the plot:

$$d\ \ln(IT)/d(1/T) = -\Delta H^{\circ}_{T}/R \qquad (9)$$

At elevated temperatures, the concentration of Mo ($^7S_3$) atoms is sufficient that self-absorption of the fluorescent radiation reduces the measured intensity. The self-absorption effect is analyzed as follows.

The concentration of absorbing atoms is:

$$n_a = C_a\ \exp(-\Delta H^{\circ}_{T,a}/RT)/T \qquad (10)$$

and the concentration of atoms from which fluorescence is induced is:

$$n_f = C_f\ \exp(-\Delta H^{\circ}_{T,f}/RT)/T \qquad (11)$$

The fluorescence intensity produced, I_0, is reduced by the self-absorption effect to the measured intensity, I:

$$I/I_0 = \exp\ (-kn_a) \qquad (12)$$

where the self-absorption coefficient, k, has been assumed constant over the relatively small temperature range in which this analysis of self-absorption will be applied. We also neglect the small variation of evaporation enthalpy and entropy over the temperature range of the experiment by assuming that $\Delta H^{\circ}_{T,a}$ and $\Delta H^{\circ}_{T,f}$ are independent of temperature. I_0 is proportional to n_f, and we obtain

$$\ln\ IT = A + B/T + C\ \exp\ (B'/T)/T \qquad (13)$$

where $B = -\Delta H^{\circ}_{T,f}/R$ and $B' = -\Delta H^{\circ}_{T,a}/R$. In the present case, B and B' are equal, and an iterative least squares analysis of the data yields the constants, A, B, and C. For the more general case, where fluorescence occurs into an energy level that differs from the one excited by the laser, the difference between B and B' is calculated from the known energy difference of the two levels.

Analysis of the molybdenum data gives $\Delta H^{\circ}_{2535} = 610 \pm 15$ kJ/g-mole and the line drawn through the data in the figure. Similar experiments with tungsten evaporation show that the self-absorption effect is accurately modeled if $I/I_0 > 0.5$. Data that do not meet this test have not been used in the data reduction procedure.

The expected evaporation enthalpy differs from that listed in tables[4,5] of thermodynamic properties ($\Delta H^{\circ}_{2535} = 633.5$ kJ/g-mole), which pertains to evaporation into an equilibrium distribution of atomic electronic states. The experiment studied evaporation into a single electronic state:

$$Mo(s) = Mo(^7S_3) \qquad (14)$$

for which accepted thermodynamic data[4,5] yield $\Delta H^o_{2535} = 633 \pm 2$ kJ/g-mole. (The difference between this and the equilibrium enthalpy of evaporation is small because molybdenum atoms display no low lying electronic states.[9])

The temperature range of the Mo vaporization study was 2293 to 2770K. The true specimen temperatures were measured with a calibrated optical pyrometer, and corrected for the known[11] temperature dependent emittance of Mo. If the pyrometer calibration error were +8K at 2293K and -9K at 2770K, the measured value of ΔH^o_{2535} would agree with the literature value. Such corrections are slightly outside the uncertainties in the pyrometer calibration (which were obtained against a calibrated tungsten filament lamp at the National Bureau of Standards). However, the precision of our enthalpy measurement, which does not include uncertainty in the pyrometer calibration, and the pyrometer calibration uncertainty easily account for the difference between the measured and literature values for Mo evaporation to the atomic $^7S_3$ state.

5. Tungsten evaporation: Preliminary tungsten evaporation results were presented in our first annual report.[1] At the time of that report, the departure of ln(IT) versus 1/T plots from a straight line at higher temperatures had not been identified as a self-absorption effect.

The electronic transitions that have been laser pumped are shown as solid lines in Figure 7. Fluorescence was collected at the pumping wavelength or from the transitions indicated by dashed lines in the figure. Intensity versus temperature data were obtained for five electronic states. A few radiative lifetimes were obtained by measuring intensity versus detection delay time. The values obtained are given in Figure 8. These results are uncertain by about ±20%.

Excellent discrimination against scattered laser radiation was achieved by delayed detection at the exciting wavelength or by monitoring fluorescence at a wavelength different from that of the laser. Delayed detection was not possible at high detector sensitivities for which the detector time constant was about 2 μs. Then good scattered light rejection was achieved if the light trap opposite the window through which fluorescence was collected was kept clean.

Figure 9 presents intensity versus temperature data for tungsten ground ($^5D_0$) state atoms at three different argon pressures. LIF from the $^5F^o_1$ state was used in these experiments. Sensitivity is greater at the higher pressure because the tungsten atoms diffuse less rapidly. The concentration in the immediate wake of the filament, where LIF was produced, is then larger. The reduction in self-absorption effects at lower pressures is much greater than can be explained by reduced concentration-distance product in the region that fluorescence must pass through. At low pressures, the W-atom mean free path is about equal to the distance from the filament to the point of LIF. Then, the velocity vectors of the atoms detected differ from those of the absorbing atoms, and the self-absorption effects are reduced by the doppler shift between the fluorescence and absorption lines.

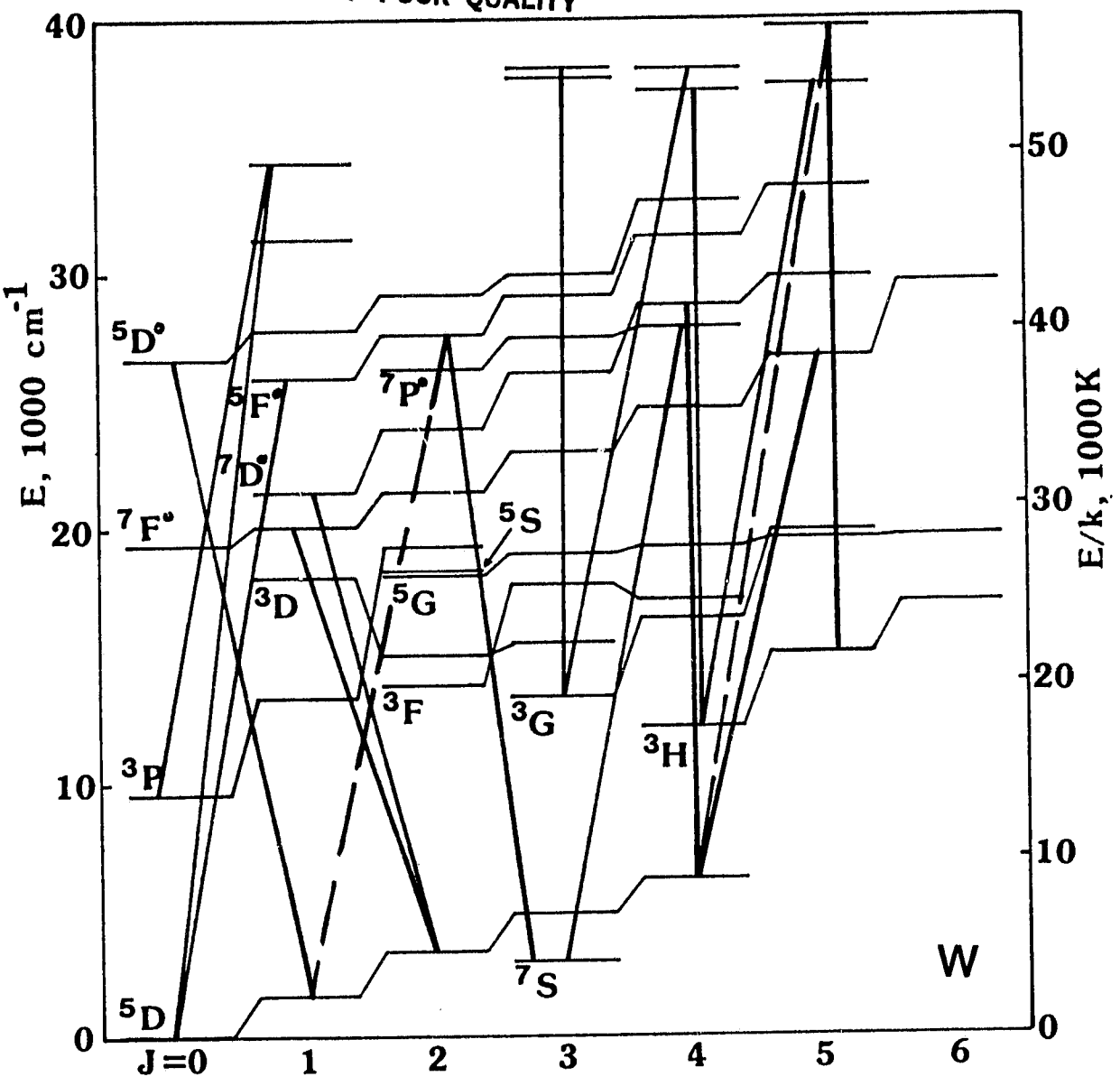

Figure 7 - Partial Energy Level Diagram for Atomic Tungsten. The solid lines indicate transitions that were laser pumped. The dashed lines are the transitions used to monitor fluorescence induced in $^{7}S_{3}$ and $^{3}H_{5}$ atoms.

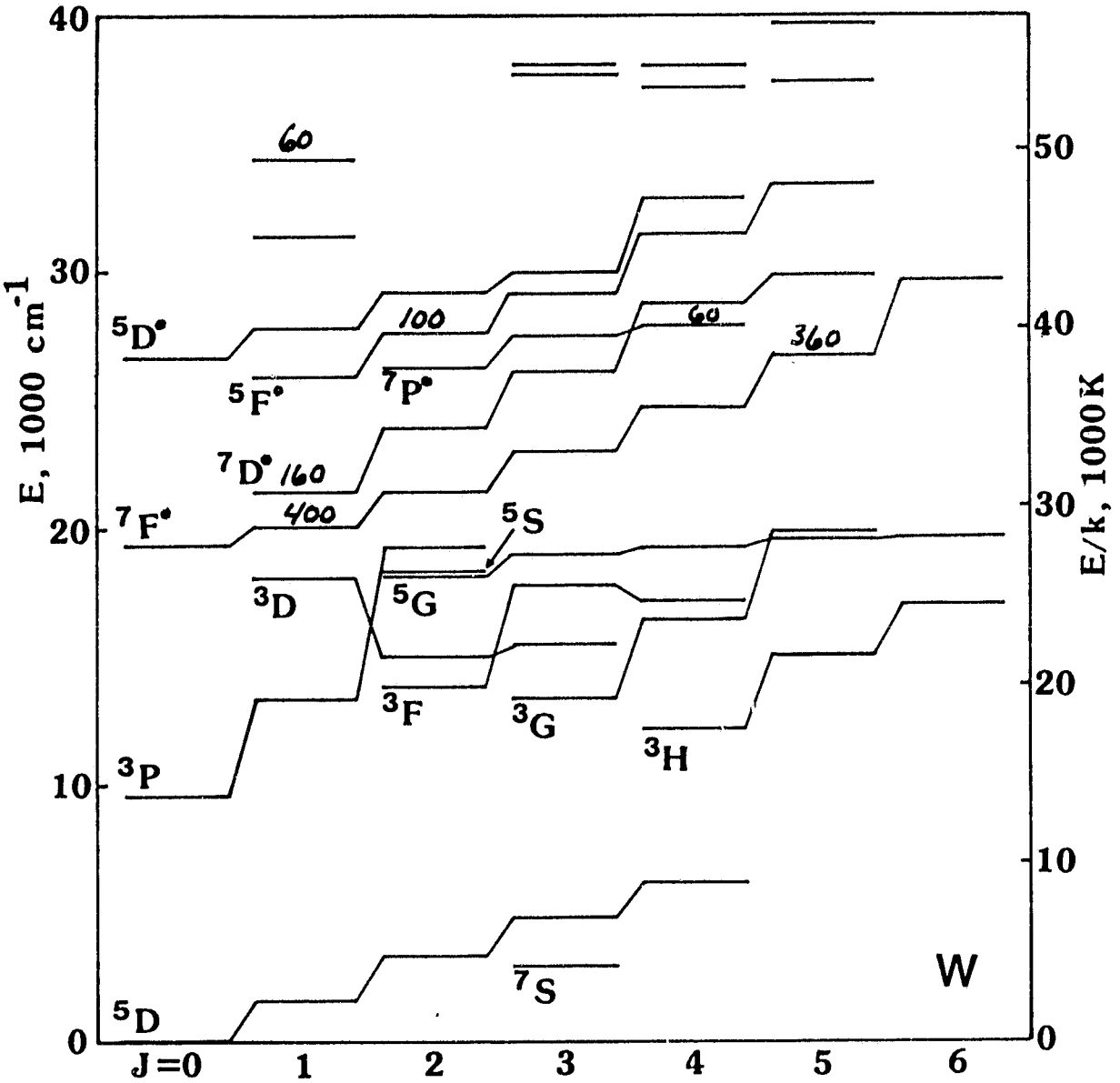

Figure 8 - Radiative Lifetimes for Atomic Tungsten. The values (in ns) are uncertain by about ± 20%.

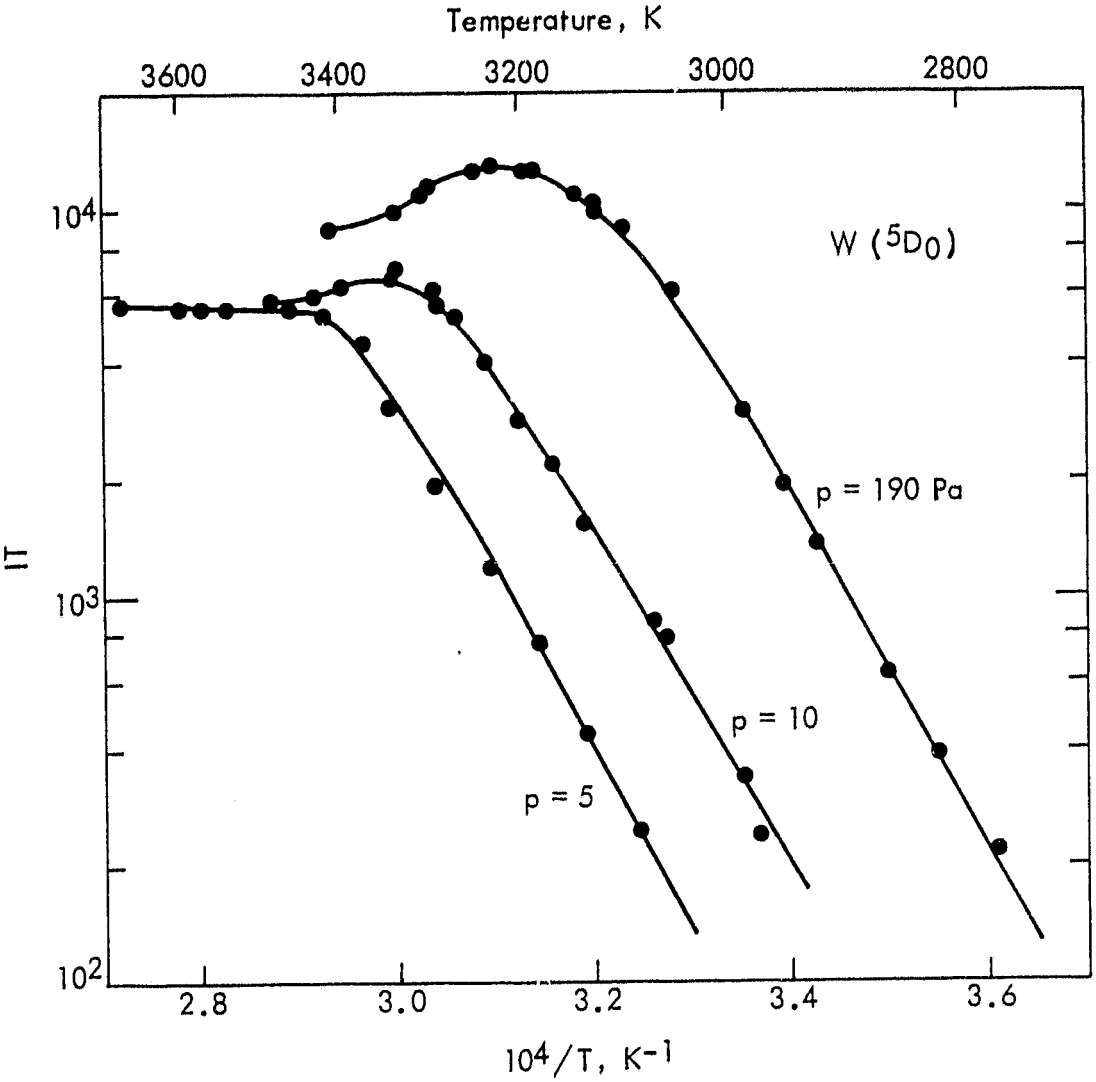

Figure 9 - Temperature Dependence of Fluorescence Intensity for W ($^5D_0$) Ground State Atoms in the Wake of an Electrically Heated Tungsten Filament. Different pressures of flowing argon gas (velocity $\cong$ 30 m/s) were used for the three experiments.

Figure 10 repeats the data from Figure 9 at p = 190 Pa and presents results for four other metastable electronic states. (All levels below the $^7F^o$ states are even levels, for which the sum of electron angular momentum quantum numbers is even, and are metastable.)

Figure 7 shows that fluorescence detection of $^3P_0$ and $^5D_0$ atoms can be achieved by use of common upper level at E = 34,342 cm^{-1}. In a single experiment, fluorescence from the 34,342 cm^{-1} to $^5D_0$ states was used to measure $^3P_0$ and $^5D_0$ concentrations. No change in the experimental geometry occurred between the two sets of intensity measurements and nearly identical self-absorption effects should thus be obtained. The intensity ratios would then be free from self-absorption effects. Figure 11 presents the results, with the $^3P_0$:$^5D_0$ intensity ratios plotted at the bottom of the figure. The expected absence of self-absorption effects in the intensity ratios is obtained. The $^5D_0$ to $^3P_0$ excitation energy derived from the slope of the ratio plot is 110 ± 18 kJ/g-mole, in good agreement with the spectroscopic value (114.0 kJ/g-mole) for this energy.

Table 3 presents the enthalpies of evaporation calculated from the several experiments at p = 190 Pa. The table lists the metastable electronic state that was studied, its electronic excitation energy, and the enthalpy of tungsten evaporation into this state as calculated from Eq. (13). The difference between the evaporation enthalpy and the electronic excitation energy is the enthalpy of evaporation to ground state atoms, which is given in the last column. The average enthalpy of evaporation to the $^5D_0$ ground state at ($\bar{T}$ = 3120K) is 861 kJ/g-mole and the average deviation of the seven measurements is 24 kJ/g-mole. The literature value[4] for this quantity is 824 ± 4 kJ/g-mole. (The enthalpy of evaporation[4] to an equilibrium distribution of W-atom electronic states is 859 kJ/g-mole at 3120K.)

The pyrometer was calibrated in the range of these experiments by observing the apparent melting temperatures of tungsten and molybdenum filaments, with a precision ca. ± 10K. An additional error in the pyrometer calibration results from uncertainty in the melting point of W (3680 ± 20K)[5] and Mo (2890K[4] or 2892 ± 10K[5]). The difference between the measured and literature values for the enthalpy of tungsten evaporation is within the error that may result from pyrometer calibration uncertainty and the enthalpy measurement precision.

However, repeat measurements of the $^5D_0$ and $^3P_0$ evaporation enthalpies differ by amounts larger than the statistical errors in the derived ΔH values. It is thus apparent that systematic errors between experiments are significant, and the difference between the experimental results and literature values are probably also due to systematic errors. One such error arises because the experiments are carried out in argon. The gas temperature and density in the wake of the filament differ from the values at the filament. Thus, density at the point at which fluorescence was measured is not strictly proportional to the vapor density at the filament. This problem does not occur for vacuum evaporation experiments and may be eliminated in the present work by measuring atom concentration versus distance from the evaporating surface.

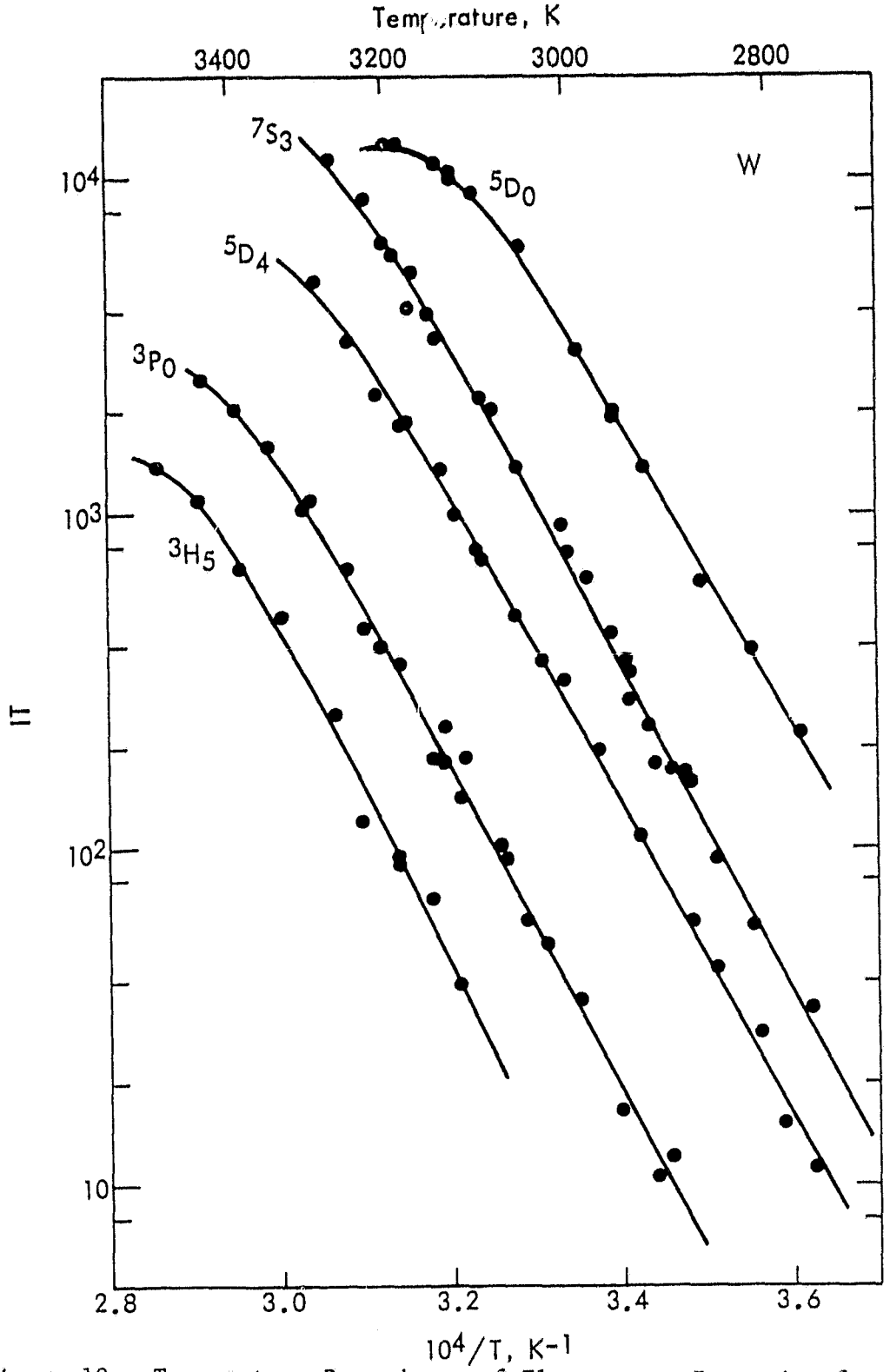

Figure 10 - Temperature Dependence of Fluorescent Intensity for Five Electronic States of Atomic Tungsten in the Wake of Electrically Heated Tungsten Filaments. The argon flow velocity was about 30 m/s at p = 190 Pa.

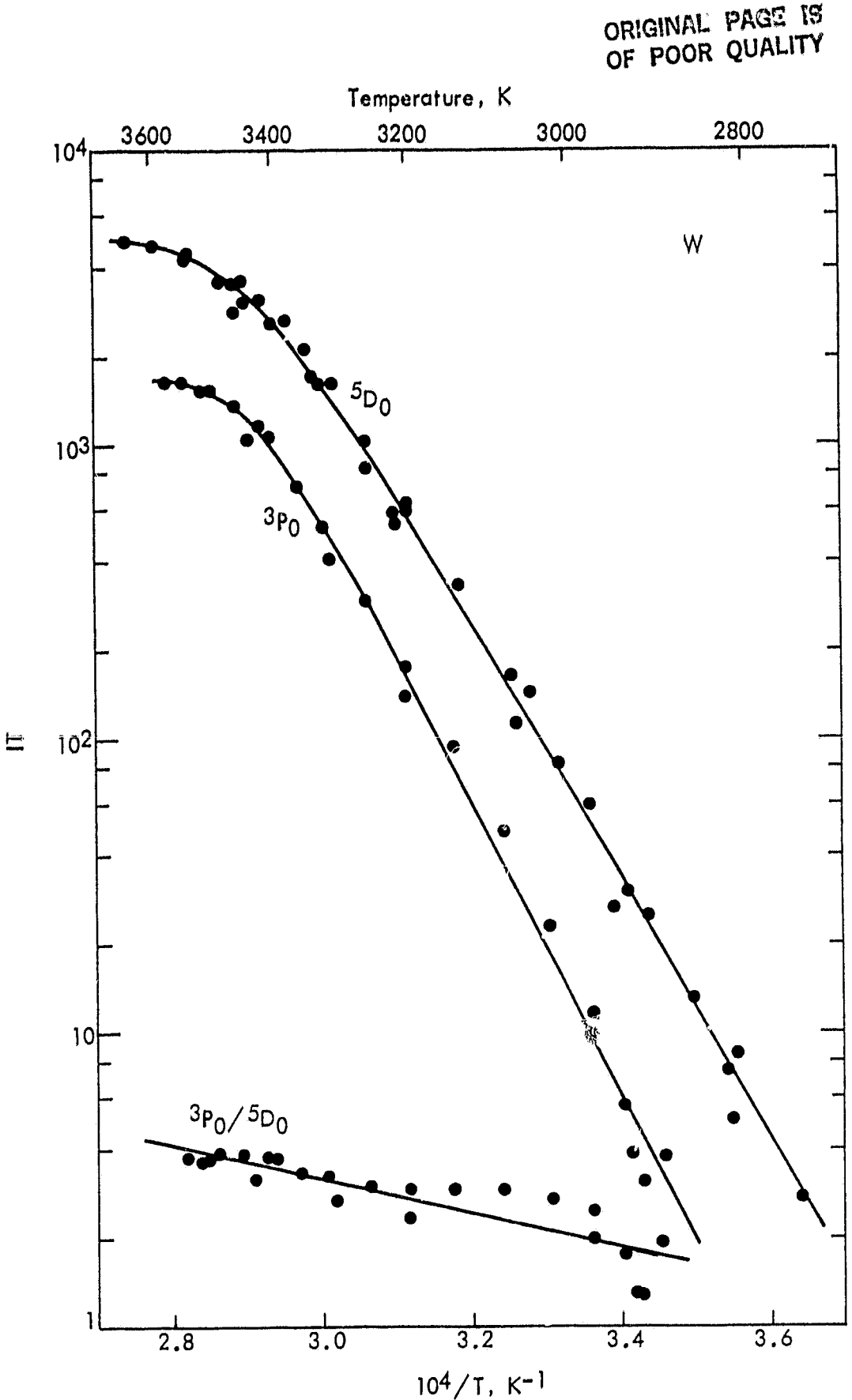

Figure 11 - Measurement of the ^3P_o:^5D_o Fluorescence Intensity Ratio. Both states were excited to the E - 34,342 cm^{-1} electronic state and fluorescence into the ^5D_o state was observed at λ = 291.1 nm. Self absorption effects occur at high temperatures but do not influence the calculated intensity ratios.

TABLE 3

TUNGSTEN FILAMENT EVAPORATION RESULTS

Atomic State	Energy kJ/g-mole	Evaporation Enthalpies, kJ/g-mole	
		Measured State	Ground State
$^5D_0$	0	858	858
$^5D_0$	0	896	896
$^7S_3$	35	939	904
$^5D_4$	74	900	826
$^3P_0$	114	945	831
$^3P_0$	114	983	869
$^3H_5$	180	1,025	845
		Average Value	861
		Average Deviation	24
		Literature Value	824 ± 4

Figure 12 presents W^+ intensity versus temperature data, obtained by exciting the $^6D_{1/2}$ ground state of ionic tungsten to the $^6F^o_{3/2}$ level at λ = 255.5 nm. With Eq. 13, we calculate ΔH^o_{3130} = 855 ± 11 and ΔH^o_{3300} = 817 ± 37 kJ/g-mole from the data at p = 190 and p = 5 Pa, respectively.

The tungsten ion evaporation reaction is

$$W(s) = W^+ + e^- \tag{15}$$

and the reaction investigated is

$$W(s) = W^+(^6D_{\frac{1}{2}}) + e^- \tag{16}$$

We assume that the total W^+ ion and the electron concentrations are equal. Then for reactions (15) and (16)

$$d\ \ln(p_e)^2/d(1/T) = -\ \Delta H^o_{15}/R \tag{17}$$

$$d\ \ln[P_e P_{W+(^6D_{1/2})}]/d(1/T) = -\ \Delta H^o_{16}/R \tag{18}$$

and

$$-Rd\ \ln(IT)/d(1/T) = (\Delta H^o_{16} - \Delta H^o_{15}/2), \tag{19}$$

which equals 812 and 810 kJ/g-mole at 3130 and 3300K, respectively. Good agreement with the literature is thus obtained for the low pressure experiment where the assumed proportionality between intensity and concentration is valid. The experiments at p = 190 Pa yield an evaporation enthalpy that exceeds the literature value by about the same fraction found in the W-atom evaporation results.

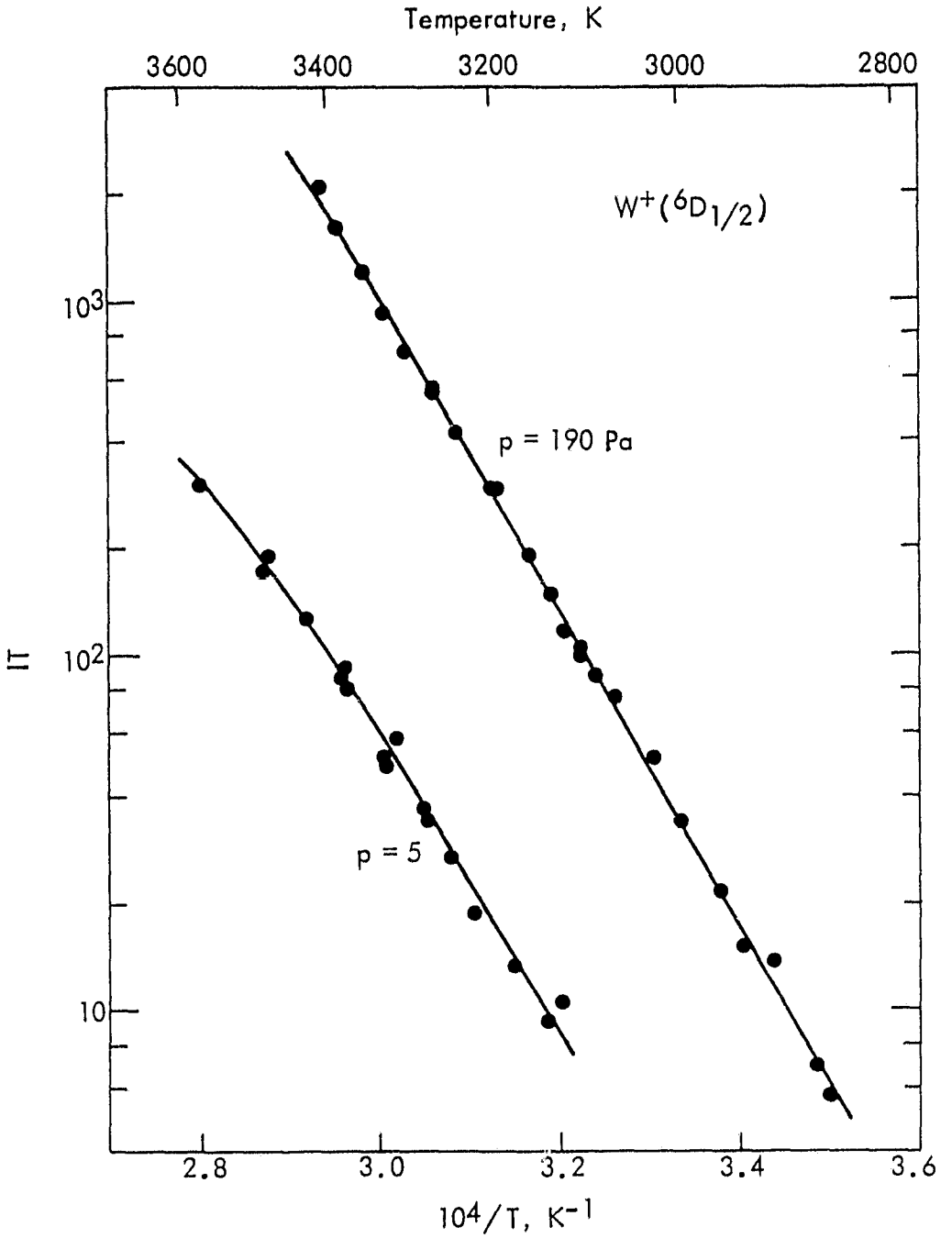

Figure 12 - Temperature Dependence of the Tungsten Ion Ground State Fluorescence Intensity in the Wake of an Electrically Heated Tungsten Filament. The argon flow velocity was 30 m/s at the indicated pressure.

IV. DISCUSSION

The results obtained demonstrate several new methods by which LIF can be used for containerless high temperature property measurements and process control. Experience also indicates a number of improvements or changes that would be useful in earth or space based research. Accurate temperature measurement and control is a critical requirement in such research, which cannot be satisfied by optical pyrometry if specimen emittances have not been independently measured or change during an experiment or process.

Three new methods for temperature measurement can be evaluated on the basis of the current results. These methods use LIF measurements of gas density, atomic electronic state population ratios, or the velocities of evaporating atoms to determine temperature. The velocity measuring technique is applicable in vacuum and the gas density method requires an inert ambient atmosphere. The calculation of temperatures from electronic state population ratios or velocities requires the assumption that the gas is in thermal equilibrium with the hot surface of interest. The two techniques provide a check on this assumption because they would yield equal temperatures only by coincidence if the assumption was not correct.

Mercury is a convenient nonreactive, volatile seed gas for LIF gas density thermometry. However, thermal diffusion of Hg atoms in lighter gases has a large influence on the concentration gradients that develop in a nonisothermal gas. The rates of convective mass and heat transfer also influence temperature and concentration gradients, and the technique is therefore not easily applied in earth-based experiments. In space, convective effects can be avoided in containerless nonisothermal experiments and accurate calibration of Hg-atom LIF gas density thermometry may be achieved. Also, the smaller temperature gradients that obtain in the absence of convective heat transfer would allow a considerable improvement of the ±3% precision in temperature that was achieved in our experiments.

Accurate electronic state population ratios can be measured even when self absorption effects influence the relation between intensity and concentration (c.f., Figure 11). However, the precision of the ratios obtained in the current work is reduced by the need to calculate them from separate measurements of intensity versus temperature for the two species of interest. The precision of temperature measurement then influences the precision of the ratio measurements. For example, assume that the $^5D_0$ intensity versus temperature function is known exactly and that te $^3P_0$ LIF intensity is measured at a temperature uncertain by ±10K. At 3500K, the appropriate $^5D_0$ intensity by which the $^3P_0$ intensity should be divided is then uncertain by about 17%. Simultaneous measurements of the two intensities (with two lasers) would eliminate this effect and allow more precise population ratio measurements.

The equilibrium tungsten $^3P_0$:$^5D_0$ population ratio, R, is

$$R = \exp\,[-13713/T(K)] \tag{20}$$

and the temperature may be calculated from measurements of R with a precision

$$\Delta R/R = (13713/T)(\Delta T/T) \tag{21}$$

R measurements to ±1% should be possible by two laser techniques and at 3500K, the temperature would then be fixed to ±9K. Appropriate calibration of the intensity ratio measurements would allow absolute temperatures to be calculated, with an accuracy and precision equivalent to that of optical pyrometry.

Velocity thermometry relates the mean thermal speed, c, of evaporating atoms to the surface temperature via

$$c = (8kT/\pi m)^{\frac{1}{2}} \tag{22}$$

with a precision

$$\Delta c/c = 0.5(\Delta T/T) \tag{23}$$

Comparison of Eqs. 21 and 23 at, say, 3500K shows that the precision of velocity measurements must exceed that of electronic population ratios by about eight times if the two methods are to yield equally precise temperatures. On the other hand, no calibrations are required to obtain absolute temperatures from velocity thermometry.

We obtained[1] a supersonic levitation jet velocity equal to 394 ± 24 m/s by measuring the fluorescence image position versus the delay time between the laser pulse and fluorescence detection. The low precision of this measurement is mainly due to the ±0.001 cm uncertainty in position measurements and the small image motion in the delay times interval (240 ns, twice the Hg atom radiative lifetime) for which fluorescence was observable. We estimate that the velocity of evaporating tungsten atoms at 3500K could be measured to about ±1% by observing time delayed fluorescence from the 400 ns $^7F_1^o$ state. However, a spatial filter would be necessary to improve the focusing properties of the visible dye laser beam and more sensitive detection electronics would be necessary for such experiments.

A more sensitive and more widely applicable method for velocity measurements that does not require a large upper electronic state lifetime employs two lasers. Consider, for example, the transitions between tungsten $^3P_0$ or $^5D_0$ atoms and the upper energy level at E = 34,342 cm^{-1}. About 30% of the $^5D_0$ atoms pumped to this level fluoresce to the $^3P_0$ state. A focused laser pulse at λ = 291.1 nm would thus create a high concentration of metastable $^3P_0$ atoms in the region it intercepts. A subsequent laser pulse at λ = 402.9 nm would re-excite the $^3P_0$ atoms to the 34,342 cm^{-1} level and about half of the resulting fluorescence would occur at λ = 291.1 nm. The time delay between the two laser pulses can be chosen to give, say, a 1 cm

average displacement of $^3P_0$ atoms between creation and detection. The resulting velocity measurements would not be limited by spatial resolution effects, and can probably be made to much better than ±1%.

The difference between measured and literature values for the enthalpies of Mo and W evaporation were within the uncertainty of the measurements and of the optical pyrometer calibrations. These differences are, nevertheless, much larger than typical errors in the enthalpies of formation of many refractory materials. This is because the second law technique, which derives enthalpies from the temperature dependence of an equilibrium constant (K_{eq}) is inferior to the third law technique, which requires an absolute value of K_{eq} at a given temperature, and calorimetric measurements of the reaction entropy. In the present study of tungsten evaporation, a 10K temperature error, of opposite sign at either end of the pyrometer calibration interval (2890 to 3680K) produces a 2.7% error in the evaporation enthalpy. Even larger errors may be present due to the uncertainty in the melting points of Mo (±10K)[5] and W (±20K).[5] On the other hand, the temperature error required to produce a 2.7% error in the 3rd law enthalpy for tungsten evaporation is nearly 100K at 3400K if there is no error in the equilibrium constant measurement. If the temperature is exactly measured to be, say, 3400K, a 2.3-fold error in the equilibrium constant would produce a 2.7% error in the evaporation enthalpy.

With accurate temperature measurements, which we have shown possible, containerless LIF experiments can achieve accurate third law measurements of reaction enthalpies. For binary compounds, the required data are activities of the elemental components. The activities can be directly measured by LIF as the ratio of fluorescence intensities over the material of interest and over the pure elements at the same temperature. Gas phase/condensed phase equilibrium is required and would be achieved in vacuum evaporation experiments only for materials whose evaporation coefficients are unity. Unit evaporation coefficients are typical of metals and liquids. Thus, application of LIF to thermodynamic measurements on high temperature liquids is a promising application for containerless experiments.

Gas phase/condensed phase equilibrium can be insured by use of an ambient inert gas atmosphere that retards the evaporation rate. In spherical geometry, with a large container to specimen radius ratio, the diffusion limited evaporation rate, f, is

$$f_D = 2Dn/d \tag{24}$$

where $n = p/RT$ (p is the equilibrium vapor pressure), D is the binary diffusivity of the vapor specie in the ambient atmosphere, and d is the specimen diameter. In Knudsen effusion,

$$f_K = nca/4A \tag{25}$$

where $c = (8kT/\pi m)^{\frac{1}{2}}$ is the mean thermal speed of evaporating atoms or molecules and a/A is the ratio of effusion cell orifice area to the specimen surface area. Typical values are $a/A = 0.01$, $c = 5 \times 10^4$ cm/s, $d = 0.3$ cm,

and D = 1 cm^2/s (at, say, p = 1 atm and T = 2000K). Then, if the ambient pressure exceeds 0.05 atm, the rate of diffusion limited evaporation in the containerless experiment would be less than the rate of evaporation from a typical Knudsen effusion cell. Gas phase/condensed phase equilibrium should thus be easily obtained and verified by use of an inert gas to suppress evaporation by an amount that depends on the inert gas pressure.

V. REFERENCES

1. Nordine, P. C. and R. A. Schriftman, "Containerless High Temperature Property Measurements by Atomic Fluorescence," Annual Technical Report, NASA Contract NAS8-34383, Yale University, New Haven, Connecticut, October 1982.

2. Nordine, P. C. and R. M. Atkins, "Aerodynamic Levitation of Laser-Heated Solids in Gas Jets," Rev. Sci. Instrum., 53, 1650 (1982).

3. Nordine, P. C., R. A. Schriftman, and D. S. Sethi, "Atomic Fluorescence Study of High Temperature Aerodynamic Levitation," in G. E. Rindone, ed., Materials Processing in the Reduced Gravity Environment of Space, Elsevier, New York, 1982, pp. 43-48.

4. Hultgren, R., P. D. Desai, D. T. Hawkins, M. Gleiser, K. K. Kelley, and D. D. Wagman, "Selected Values of the Thermodynamic Properties of the Elements," Am. Soc. for Metals, Metals Park, Ohio (1973).

5. Stull, D. R. and H. Prophet, JANAF Thermochemical Tables, 2nd Ed., USGPO, Washington, D.C. (1971); M. W. Chase, J. L. Curnutt, R. A. McDonald, and A. N. Syverud, J. Phys. Chem. Ref. Data, 7, 793-940 (1978).

6. Grynak, D. A. and D. E. Burch, "Optical and Infrared Properties of Al_2O_3 at Elevated Temperatures," J. Opt. Soc. Amer., 55, 625-629 (1965).

7. Nordine, P. C., E. H. Lee, and J. L. Hurd, "Spectral Emittance of Polycrystalline Alumina," Rev. int. hautes Temper. Refract., 17, 165-171 (1980).

8. Bier, K. and B. Schmidt, Z. Angew. Phys., 13, 34 (1961); H. Ashkenas and F. S. Sherman, Proc. 4th Int. Symp. on Rarefied Gas Dynamics, J. H. Deleeuw, ed., Academic Press, New York (1966), Vol. 2, p. 84; S. Christ, P. M. Sherman, and D. R. Glass, AIAA J., 4, 68 (1966).

9. Moore, C. E., Atomic Energy Levels, I, II, III, USGPO Washington, D.C. (1971).

10. Meggers, W. F., C. H. Corliss, and B. F. Scribner, Tables of Spectral-Line Intensities Part I - Arranged by the Elements, NBS Publication NN-145, USGPO, Washington, D.C., 1975.

11. Espe, W., Materials of High Vacuum Technology Vol. 1, Metals and Metalloids, Pergamon Press, New York (1966).

12. Van Audenhove, J., "Vacuum Evaporation of Metals by High Frequency Levitation Heating," Rev. Sci. Instrumen., 36, 383-385 (1965).

VI. PUBLICATIONS AND PRESENTATIONS

Schiffman, R. A. and P. C. Nordine, "Laser Induced Fluorescence Study of Al_2O_3 Evaporation and High Temperature Gas Thermometry" (in preparation).

Nordine, P. C. and R. A. Schiffman, "Laser Induced Hg ($^3P_1$) Fluorescence Study of a Supersonic Free Jet," (in preparation).

Nordine, P. C., "Chemical Reaction Studies with Laser Induced Fluorescence," presented at the NASA Containerless Processing Meeting, Arlington, Virginia, October 21-22, 1982.

Nordine, P. C., "Containerless High Temperature Property Measurements by Laser Induced Fluorescence," Materials Science in Space Seminar, Presented at NASA-Lewis Research Laboratory, November 3, 1982.

Schiffman, R. A. and P. C. Nordine, "Pulsed Laser Fluorescence Study of Evaporating Metals," Presented at the 1983 TMS-AIME Annual Meeting, Atlanta, Georgia, March 6-10, 1983.

Nordine, P. C., "Laser Induced Atomic Fluorescence Studies of High Temperature Systems," Presented at Midwest Research Institute, Kansas City, Missouri, March 17, 1983.

Nordine, P. C. and R. A. Schiffman, "Laser Induced Fluorescence Study of Reactions on Levitated Materials," Presented at the Midwest High Temperature Chemistry Conference, Lawrence, Kansas, June 9-11, 1983.

Schiffman, R. A., "Temperature Measurement by Laser Induced Fluorescence," Presented at the Midwest High Temperature Chemistry Conference, Lawrence, Kansas, June 9-11, 1983.

Nordine, P. C., "Laser-Induced Fluorescence Studies of Ceramics at High Temperatures," to be presented at Lawrence Livermore National Laboratory, Livermore, California, July 18, 1983.